

# Exploiting the Unique ATP-Binding Pocket of *Toxoplasma* Calcium-Dependent Protein Kinase 1 To Identify Its Substrates

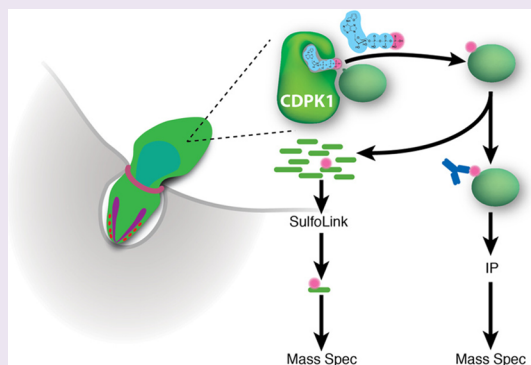
Sebastian Lourido,<sup>†,§</sup> Grace R. Jeschke,<sup>‡</sup> Benjamin E. Turk,<sup>‡</sup> and L. David Sibley<sup>\*,†</sup>

<sup>†</sup>Department of Molecular Microbiology, Washington University School of Medicine, 660 S. Euclid Ave., St. Louis, Missouri 63110, United States

<sup>‡</sup>Department of Pharmacology, Yale University School of Medicine, 333 Cedar St., New Haven, Connecticut 06520, United States

## S Supporting Information

**ABSTRACT:** Apicomplexan parasites rely on calcium as a second messenger to regulate a variety of essential cellular processes. Calcium-dependent protein kinases (CDPK), which transduce these signals, are conserved among apicomplexans but absent from mammalian hosts, making them attractive targets for therapeutic intervention. Despite their importance, the signaling pathways CDPK regulate remain poorly characterized, and their protein substrates are completely unknown. In *Toxoplasma gondii*, CDPK1 is required for calcium-regulated secretion from micronemes, thereby controlling motility, invasion, and egress from host cells. CDPK1 is unique among parasite and mammalian kinases in containing glycine at the key “gatekeeper” residue, which results in an expanded ATP-binding pocket. In the present study, we use a synthetic ATP $\gamma$ S analogue that displays steric complementarity to the ATP-binding pocket and hence allows identification of protein substrates based on selective thiophosphorylation. The specificity of this approach was validated by the concordance between the identified phosphorylation sites and the *in vitro* substrate preference of CDPK1. We further demonstrate that the phosphorylation of predicted substrates is dependent on CDPK1 both *in vivo* and *in vitro*. This combined strategy for identifying the targets of specific protein kinases provides a platform for defining the roles of CDPKs in apicomplexans.



Apicomplexan parasites cause prevalent and deadly human infections, with up to a quarter of the world's population chronically infected with *T. gondii*<sup>1</sup> and nearly a million deaths annually due to malaria, caused by *Plasmodium* spp.<sup>2</sup> Their divergence from model organisms, combined with their strict parasitic lifestyle, has limited our understanding of apicomplexans and hindered the identification of novel therapeutic targets. Calcium-dependent protein kinases (CDPKs) have garnered significant attention in recent years because of their importance to parasite biology and their absence from mammalian hosts.<sup>3</sup>

Host cell invasion by apicomplexan parasites depends on gliding motility, which relies on apically secreted adhesins for substrate-dependent forward movement.<sup>7</sup> Adhesins are translocated via actomyosin motor complexes anchored in a network of cisternae under the plasmalemma, called the inner membrane complex.<sup>8</sup> Elevated cytosolic calcium triggers release of adhesins from small, elongated vesicles, called micronemes.<sup>9</sup> Cytosolic calcium has been observed to oscillate during motility,<sup>10</sup> and movement is effectively blocked by calcium chelators.<sup>9</sup>

Calcium signaling in mammalian cells typically leads to downstream activation of protein kinase C (PKC) and calcium/calmodulin dependent protein kinase (CaMK).<sup>11,12</sup> In contrast, apicomplexans lack PKC and have few CaMK isoforms and instead express an expanded family of calcium-dependent

protein kinases (CDPKs).<sup>3,13</sup> Composed of a serine/threonine kinase domain followed by a C-terminal regulatory domain consisting of four EF hands, CDPKs are found in apicomplexans as well as plants and ciliates.<sup>14</sup> In *Plasmodium* spp. many CDPKs are dispensable for growth in erythrocytes and have been knocked out leading to defects in later developmental stages including male gamete exflagellation,<sup>15</sup> ookinete motility,<sup>16,17</sup> and sporozoite recognition of hepatocytes.<sup>18</sup> More recently, conditional expression of CDPKs in *P. falciparum* demonstrated its role in egress from erythrocytes.<sup>6</sup> Taken together, these studies demonstrate that CDPKs play central roles in parasite biology, although their precise molecular functions have yet to be established. Using a conditional knockout, we have previously demonstrated that *T. gondii* calcium-dependent protein kinase 1 (TgCDPK1) is required for microneme secretion.<sup>4</sup> However, none of the phosphorylated proteins known to regulate secretion in animals, such as rabphilin or synapsin,<sup>19</sup> are readily identifiable in apicomplexans by BLAST searches,<sup>20</sup> and the mechanism for TgCDPK1 regulation of microneme secretion remains unknown.

Received: February 18, 2013

Accepted: March 26, 2013

Published: March 26, 2013

Unlike any other known parasite or mammalian kinase, TgCDPK1 harbors a glycine at a position in the ATP-binding pocket, termed the gatekeeper, which forms a deep hydrophobic pocket.<sup>21</sup> We and others have exploited this feature to inhibit TgCDPK1 *in vitro* and *in vivo*, using bulky pyrazolo[3,4-*d*]pyrimidine (PP) derivatives originally designed to inhibit yeast or mammalian kinases that were engineered to contain a small gatekeeper.<sup>4,5,21–23</sup> Mutation of the gatekeeper residue of TgCDPK1 to a methionine prevents inhibition by PP analogues, demonstrating the specificity of these compounds in parasites.<sup>4</sup> In the current study, we used bulky ATP $\gamma$ S analogues<sup>24</sup> to detect and identify the protein substrates of TgCDPK1. This work serves to emphasize the potential of chemical genetics in investigating both the phenotypes and cellular pathways regulated by essential kinases in parasites.

## RESULTS AND DISCUSSION

**TgCDPK1 Thiophosphorylates Heterologous Substrates.** Bulky ATP analogues have previously been used to specifically label the targets of kinases engineered to contain small gatekeepers.<sup>25</sup> By replacing the  $\gamma$ -phosphate of these artificial ATP-analogues with a thiophosphate, the targets of such kinases can be isolated on the basis of chemistry specific to the thiol group.<sup>24,26</sup> To utilize this strategy to study the targets of TgCDPK1, we incubated recombinant CDPK1 harboring either the wild type glycine or a methionine gatekeeper with dephosphorylated myelin basic protein (dMBP), a heterologous substrate. The following bulky ATP analogues were compared for labeling: N6-benzyladenosine-5'-O-[3-thiotriphosphate] (BTP $\gamma$ S), N6-furfuryladenosine (kinetin)-5'-O-[3-thiotriphosphate] (KTP $\gamma$ S), or N6-[2-phenylethyl]adenosine-5'-O-[3-thiotriphosphate] (PTP $\gamma$ S). Thiophosphorylation of dMBP was detected following alkylation with *p*-nitrobenzyl mesylate (PNBM) using an antibody that specifically recognizes alkylated thiophosphates (rabbit mAb 51-8).<sup>24</sup> We observed that only KTP $\gamma$ S was efficiently utilized by wild type TgCDPK1 to thiophosphorylate dMBP in a calcium-dependent manner (Figure 1, panels a,b). The ability of TgCDPK1 to utilize KTP $\gamma$ S depended on the presence of a glycine gatekeeper (CDPK1<sup>G</sup>) since the mutant kinase (CDPK1<sup>M</sup>) was unable to thiophosphorylate dMBP (Figure 1, panel a), despite the fact that this mutant enzyme is fully active when using ATP.<sup>4,5</sup> On the basis of these results, KTP $\gamma$ S was chosen for subsequent experiments to specifically identify TgCDPK1 substrates.

**Visualizing CDPK1 Targets in *T. gondii* Lysates.** To detect targets of TgCDPK1 in parasite lysates, we compared thiophosphorylation in wild type parasites (CDPK1<sup>G</sup>) and a mutant TgCDPK1 allele with a methionine at the gatekeeper position (CDPK1<sup>M</sup>).<sup>5</sup> Parasite lysates were incubated in a reaction buffer containing KTP $\gamma$ S and either 0 or 10  $\mu$ M free calcium, alkylated with PNBM, and resolved by SDS-PAGE, followed by Western blotting for thiophosphorylation or GRA1, a dense granule protein used as a loading control. Thiophosphorylated proteins were significantly more abundant in the lysates from the strain harboring CDPK1<sup>G</sup> (Figure 2, panel a), and as expected this reaction was only seen in the presence of calcium (Figure 2, panel a).

To isolate targets of TgCDPK1 from the complex lysate, we used the rabbit mAb 51-8 to immunoprecipitate thiophosphorylated proteins following alkylation. Lysates from CDPK1<sup>M</sup> expressing parasites were used as a control for nonspecific labeling. The immunoprecipitated proteins were

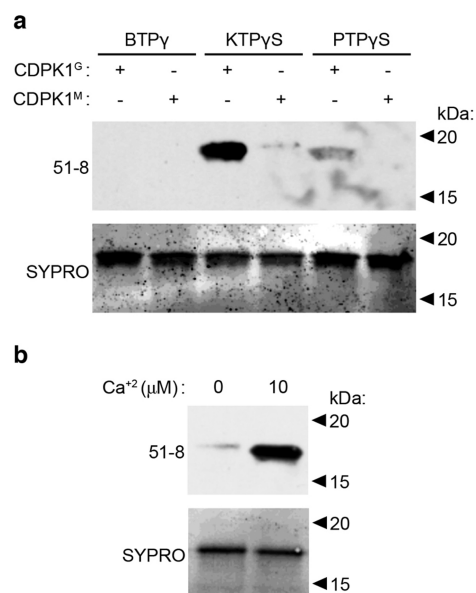


**Figure 1.** Calcium dependent protein kinase 1 (CDPK1)-dependent thiophosphorylation of a heterologous substrate using specific substrates. (a) Thiophosphorylation of dephosphorylated myelin basic protein (dMBP) by either wild type (CDPK1<sup>G</sup>) or mutant (CDPK1<sup>M</sup>) kinases using different ATP $\gamma$ S analogues. Thiophosphorylation was detected using an antibody specific for the modification (rabbit mAb 51-8), and total protein was stained with SYPRO Ruby. (b) Thiophosphorylation of dMBP by CDPK1<sup>G</sup> using KTP $\gamma$ S in the presence of either 0 or 10  $\mu$ M free Ca<sup>2+</sup>.

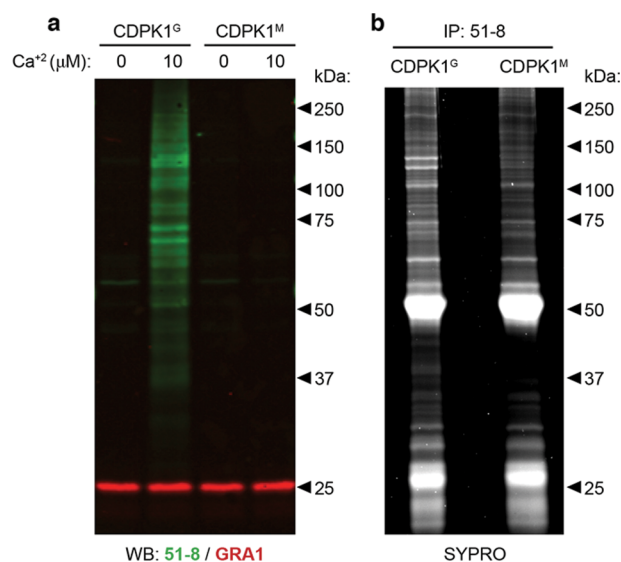


**Figure 2.** Thiophosphorylation and isolation of CDPK1 targets in *T. gondii* lysates. (a) Thiophosphorylated substrates in permeabilized parasites expressing either CDPK1<sup>G</sup> or CDPK1<sup>M</sup>, in the presence of either 0 or 10  $\mu$ M free Ca<sup>2+</sup> and KTP $\gamma$ S. On the same blot, thiophosphorylation was detected with the specific antibody (51-8; green), and detection of the dense granule protein GRA1 (red) was used as a loading control. (b) Immunoprecipitation (IP) of thiophosphorylated substrates using the specific antibody 51-8 from parasites expressing either CDPK1<sup>G</sup> or CDPK1<sup>M</sup>. Total protein was stained with SYPRO Ruby.

resolved by SDS-PAGE and stained with SYPRO Ruby (Invitrogen). A number of bands were specifically detected in the CDPK1<sup>G</sup> sample, potentially representing targets of

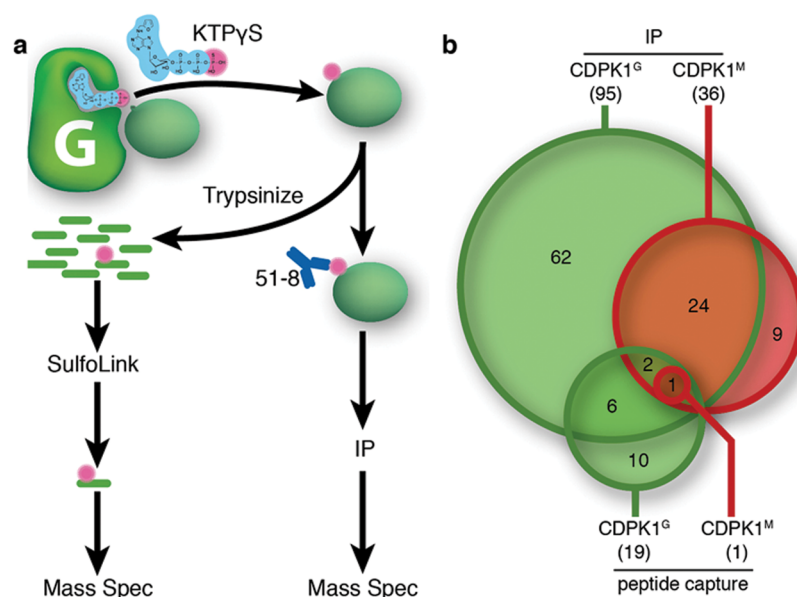


**Figure 3.** Identification of thiophosphorylated proteins. (a) Strategy for identifying thiophosphorylated targets. KTP $\gamma$ S is depicted in light blue with the  $\gamma$ -thiophosphate, transferred to substrates, highlighted in pink. Targets were either trypsinized to isolate thiophosphorylated peptides or immunoprecipitated to isolate entire proteins. (b) Diagram summarizing the numbers of proteins identified for each sample using either the IP or peptide-capture strategies and depicting the overlap between the different data sets. Total number of proteins for each data set shown in parentheses.

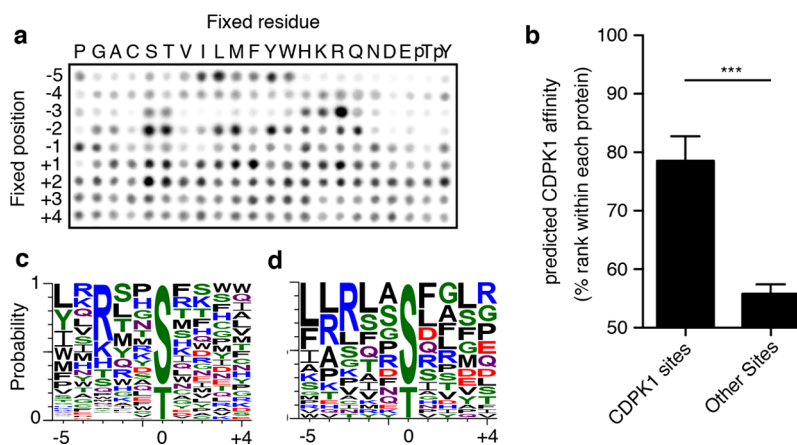


**Figure 4.** CDPK1 substrate preference. (a) Peptide array probing CDPK1 substrate preference by radiolabeled kinase assay. (b) Predicted preference of CDPK1, based on the peptide array, for identified thiophosphorylation sites (CDPK1 sites) versus sites previously identified in a global phosphoproteomic study (other sites) on each protein. Student's  $t$  test; \*\*\*,  $P < 0.0005$ ; means  $\pm$  SEM. Sequence WebLogo based on the peptide array (c) or the identified thiophosphorylation sites (d). Phospho-acceptor site at position 0, and height is reflective of probability.

TgCDPK1 (Figure 2, panel b). In particular, two bands between 100 and 150 kDa were observed by both immunoprecipitation and when probing the entire lysate for thiophosphorylated proteins. However, given the complexity of the thiophosphorylation patterns, we opted for a global approach rather than analyzing specific bands.

**Identifying Proteins Thiophosphorylated by TgCDPK1.** Two strategies have been described to enrich for thiophosphorylated targets and to enable their identification by mass spectrometry (Figure 3, panel a). As described above, the monoclonal antibody specific for the thiophosphorylation modification was used to immunoprecipitate target proteins.<sup>24</sup> Alternatively, the samples are digested to yield peptides and captured covalently with an iodoacetyl resin, which immobilizes peptides with free sulfhydryl groups.<sup>26</sup> Thiophosphorylated peptides are then removed from the resin by oxidation, leaving a phosphate group on the previously thiophosphorylated

residue. This latter approach permits identification of the protein and the site of thiophosphorylation. Both strategies were performed for the CDPK1<sup>G</sup> and CDPK1<sup>M</sup> samples, which were then submitted to MS/MS analyses. We restricted our analysis to proteins identified on the basis of at least two peptides, each with an identification probability greater than 90%, within the combined set of four samples. On the basis of these criteria, 114 proteins were identified among all four samples (Figure 3, panel b). In the immunoprecipitation experiment, 68 proteins were identified uniquely in the CDPK1<sup>G</sup> sample, 27 proteins were identified in both samples, and only 9 were identified exclusively in the CDPK1<sup>M</sup> sample. Fewer proteins overall were identified by the direct peptide capture strategy, but all of them carried phosphorylation of either a serine or a threonine. By the latter method, 19 proteins were identified exclusively in the CDPK1<sup>G</sup> sample, a single protein was found in both samples, and none were found only

Table 1. TgCDPK1 Targets Identified by Both Direct Peptide Pulldown and Immunoprecipitation

gene ID	annotation	MW (kDa)	phosphopeptides <sup>a</sup>	homology	
				<i>P. falciparum</i>	<i>C. parvum</i>
TGGT1_004440	hypothetical	47	LGT*SGYGTIVGNGDDEQPTTTAGDAGVNR LGT*SGYGTIVGNGDDEQPTTTAGDAGVNRK	N/A	N/A
TGGT1_030680	hypothetical	16	TDT*FVERAEELMNK TDT*FVERAEELMNK	N/A	N/A
TGGT1_064650	dynamamin-related	96	ALSSS*GVFDSKASASAAK ALPNLQSFSS*FGSGEGR	PF3D7_1145400	CGD1_580
TGGT1_065330	hypothetical	69	RLFT*FLQPDAPK LFT*FLQPDAPK LFT*FLQPDAPK RLFT*FLQPDAPK LFT*FLQPDAPK	N/A	N/A
TGGT1_088710	hypothetical	86	LYS*HLSTGLKNSVSK LYS*HLSTGLK	N/A	N/A
TGME49_005320	hypothetical	71	TVFESQKS*LTSTADFR TVFES*QPLQSR KDS*QTVFVSEPVSQVAHFR TVFESQKS*LTSTADFR	PF3D7_0723300	CGD3_3900

<sup>a</sup>Observed phosphorylation sites are followed by an asterisk (\*).

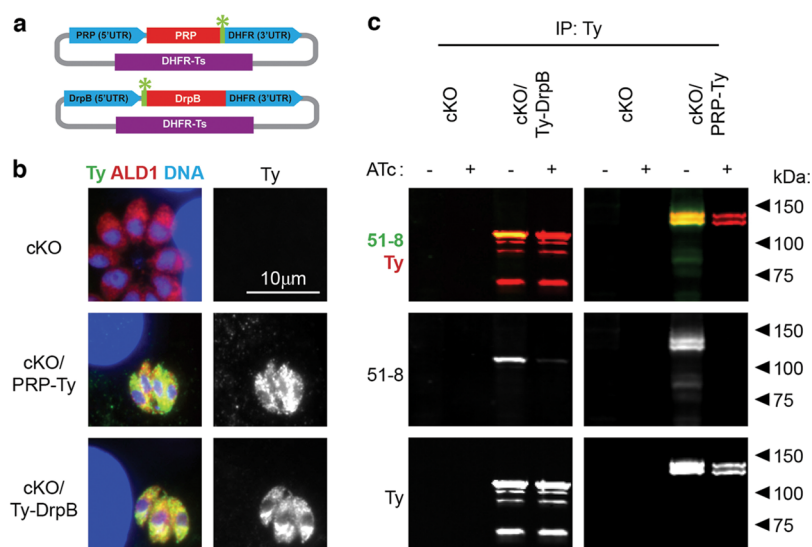


**Figure 5.** Putative targets are thiophosphorylated in a CDPK1-dependent manner. (a) Expression constructs for phosphorylated repeat protein (PRP) and dynamamin related protein B (DrpB), cloned under their endogenous 5'-UTRs with either a C-terminal or N-terminal Ty tag (Green), respectively. (b) Expression of the tagged putative targets in the CDPK1 conditional knockout (cKO) strain. Intracellular parasites were probed for *T. gondii* aldolase (TgALD1) (red), Ty (green), and DNA (blue). All images were captured at the same magnification, and the bar in the top right image gives the scale. (c) Tagged strains were grown for 72 h  $\pm$  ATc. Following thiophosphorylation, putative targets were immunoprecipitated using the Ty-tag and probed for either Ty (red) or thiophosphorylation (rabbit mAb 51-8; green).

in the CDPK1<sup>M</sup> sample (a complete list of identified proteins can be found in Supplementary Table 1). Given the low background observed by Western blotting in the CDPK1<sup>M</sup> strain (Figure 2, panel a), we speculate that many of the proteins identified for both strains in the immunoprecipitation experiment are likely enriched independently of thiophosphorylation or represent abundant proteins that are common contaminants of immunoprecipitations. In contrast the covalent capture of thiophosphorylated peptides allowed more stringent removal of background peptides, which is reflected in the data obtained by this approach. In addition to their identity, we also identified 30 distinct phosphorylation sites among the 19 proteins identified by peptide capture, which provided information about the substrate preference of TgCDPK1.

**Peptide Preference of TgCDPK1.** To explore the peptide substrate preference of TgCDPK1, we performed *in vitro* phosphorylation assays using a positional-scanning peptide array.<sup>28</sup> TgCDPK1 showed a strong preference for serine over threonine, for arginine at the  $-3$  position, and for hydrophobic residues at the  $-5$  position (Figure 4, panel a). The values from the peptide array were used to generate a protein profile, which was used to assess the preference of TgCDPK1 for each serine or threonine within the proteins identified in the CDPK1<sup>G</sup> sample by peptide capture. Although the maximum scores varied among the different proteins, we consistently observed that the highest scoring sites within each protein were those identified in the peptide capture strategy. To quantify this effect, we compared the rank within a given protein of the sites

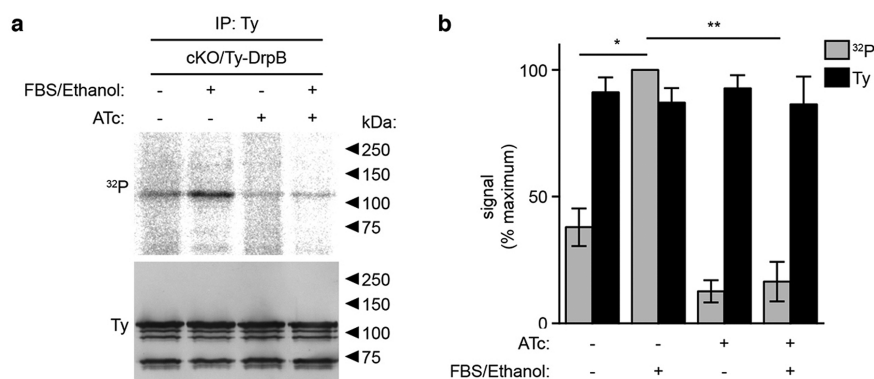


**Figure 6.** DrpB is phosphorylated *in vivo* in a CDPK1-dependent manner. (a) The TgCDPK1 cKO strain expressing Ty-tagged DrpB was grown  $\pm$  ATc for 72 h, incubated 1 h in media containing [<sup>32</sup>P] orthophosphate, and treated with either media alone or supplemented with FBS and ethanol (FBS/EtOH). Parasites were subsequently lysed, and immunoprecipitated DrpB was resolved by SDS-PAGE. Total DrpB was measured by Western blotting (Ty epitope), and radiation was measured by phosphorimaging (<sup>32</sup>P). (b) Quantitation of Western blot and radiation signals, normalized to the highest signal in each experiment. Student's *t* test; \*\*,  $P > 0.005$ ; \*,  $P > 0.05$ ; means  $\pm$  SEM,  $n = 3$  experiments.

identified as thiophosphorylated by TgCDPK1 to the rank of phosphorylation sites previously identified in a global phosphoproteome.<sup>29</sup> This analysis demonstrated a highly significant enrichment of sites preferred by TgCDPK1 among the peptides identified by thiophosphorylation and direct peptide capture in the present study (Figure 4, panel b). The similarity between the site preference of TgCDPK1 in the peptide array and that predicted by the thiophosphorylation sites is further evidenced by the similar sequence-based WebLogos generated from each data set (Figure 4, panels c and d). These observations further support the specificity of the peptide capture strategy for target identification and suggest that substrate preference by the kinase is retained under the conditions tested. They also suggest that this strategy may be useful to further define possible phosphorylation sites of candidate TgCDPK1 substrates, including those identified in the IP strategy, on the basis of the degree to which different sites match the predicted motif.

**Two Conserved Proteins Are Thiophosphorylated by TgCDPK1.** A total of six proteins were identified in both CDPK1<sup>G</sup> data sets while being absent from the CDPK1<sup>M</sup> data sets (Table 1). Of these six proteins, only one of them had been previously studied in a report that described it as a dynamin-related protein, DrpB (TGGT1\_064650).<sup>30</sup> The other five proteins were annotated as hypothetical<sup>20</sup> and had no conserved protein domains. One of the five hypothetical proteins was identified by its type II strain ME49 gene ID due to its absence from the type I strain GT1 annotation (TGME49\_005320), likely due to misannotation. Comparison of the two genomes revealed that both predicted proteins contain a central portion of repeats with a periodicity of 28 residues and that the GT1 protein is predicted to contain an additional three repeats (data not shown). Because many of the phosphorylated peptides identified came from these repeats, TGME49\_005320 will be called, henceforth, phosphorylated repeat protein (PRP).

As calcium regulation of microneme secretion is a conserved feature in apicomplexans, we predicted that crucial targets of TgCDPK1 would also be conserved, at least within the phylum. DrpB had been previously reported to be involved in the biogenesis of secretory organelles, which are lost following expression of a dominant negative mutant.<sup>30</sup> Other than DrpB, which had clear homologues in all apicomplexan genomes, only

PRP was conserved across all apicomplexans.<sup>31</sup> Despite being divergent at their N-termini, all possessed a series of 28-residue repeats in their C-termini. On the basis of their conservation among apicomplexan genomes, we decided to generate parasite strains expressing tagged versions of PRP or DrpB in order to test if they are targets of TgCDPK1 *in vivo*. We generated transgenic parasites expressing C-terminally Ty-tagged PRP or N-terminally tagged DrpB (Figure 5, panel a). Immunofluorescence analysis revealed that PRP was distributed in punctate structures throughout the cell, while DrpB was concentrated in the apical end, as previously reported.<sup>30</sup>

To determine whether TgCDPK1 was required for the thiophosphorylation, we compared the conditional knockout (cKO) of TgCDPK1 with the same strain expressing tagged versions of either DrpB or PRP. Lysates from the different strains were incubated in a reaction buffer containing KTP $\gamma$ S, and the putative targets were immunoprecipitated with the Ty-tag. Comparable amounts of both DrpB and PRP were immunoprecipitated, irrespective of the presence of anhydrotetracycline (ATc), which suppresses TgCDPK1 expression in the cKO. However, robust thiophosphorylation was detected only when strains were grown without ATc and therefore expressed TgCDPK1 (Figure 5, panel c). This result confirms that both DrpB and PRP are thiophosphorylated in a TgCDPK1-dependent manner, validating our strategy for identifying thiophosphorylated proteins.

**TgCDPK1 Regulates DrpB Phosphorylation *in Vivo*.** To confirm whether these observations could be extended to phosphorylation *in vivo*, we examined the phosphorylation of DrpB in the TgCDPK1 conditional knockout line labeled with [<sup>32</sup>P] orthophosphate and grown with or without ATc. Labeled parasites were stimulated with ethanol, which raises intracellular calcium and stimulates microneme secretion.<sup>9</sup> Equal amounts of DrpB were immunoprecipitated under all conditions. However, the amount of radiolabel incorporated into DrpB significantly increased in parasites expressing TgCDPK1 that had been stimulated to secrete (Figure 6, panel a). In contrast, when TgCDPK1 expression was suppressed by growth in ATc, labeling of DrpB was significantly reduced, regardless of stimulation (Figure 6, panel a). These differences were replicated in three independent experiments, demonstrating that DrpB is phosphorylated in a TgCDPK1-dependent manner during microneme secretion (Figure 6, panel b).

Both full-length and C-terminally truncated proteins were captured in pull-downs (Figure 6), similar to studies with DrpB and the related DrpA.<sup>30,32</sup> The observation that the truncated forms of the protein were neither thiophosphorylated (Figure 5, panel c) nor phosphorylated *in vivo* (Figure 6, panel a) indicates that modification occurs in the C terminus of DrpB, consistent with the location of sites identified by peptide capture (Table 1). This region constitutes a C-terminal extension following the GTPase effector domain, which is found in all apicomplexan DrpB homologues but not in the related DrpA,<sup>30</sup> suggesting that it might be a regulatory site specific to DrpB.

**Conclusions and Implications.** The atypical ATP-binding pocket of TgCDPK1 provides a chemical handle to distinguish its activity from that of other parasite and mammalian kinases. A bulky ATP analogue that is accommodated by the enlarged ATP-binding pocket<sup>24</sup> was used to specifically thiophosphorylate and identify protein substrates of TgCDPK1. This approach provides an unbiased method for identifying the targets of TgCDPK1, which has previously been shown to control microneme secretion during motility.<sup>4</sup> How the various targets of TgCDPK1 identified here might affect these cellular processes remains the focus of future studies. Quantitative MS approaches will also serve to confidently identify lower abundance targets, thus expanding the known repertoire of TgCDPK1 targets.

Two of the targets identified here have homologues in other apicomplexans, and we demonstrate their direct thiophosphorylation by TgCDPK1. One of these substrates, DrpB, had been previously implicated in the biogenesis of secretory organelles. Using radiolabeled parasites we were able to show that DrpB is phosphorylated *in vivo* in a TgCDPK1-dependent manner, and its phosphorylation increases when microneme secretion is triggered. Although dynamins and related proteins are typically thought of as mediating endocytosis, evidence is accumulating for a more complex role in the regulation of the vesicular trafficking dynamics, regulating the rates of vesicle recycling<sup>33</sup> and the size of fusion pores,<sup>34</sup> which may significantly restrict both the quantity and size of exocytosed material. Although further work will be needed to determine the function of DrpB phosphorylation, it is possible that the previously identified role in biogenesis of secretory organelles is only one of the functions of DrpB<sup>32</sup> and that it also plays an important role in microneme secretion.

The strategies outlined here may also be useful for comparing CDPK function across different apicomplexans, since the homologues of TgCDPK1 in *Cryptosporidium* spp. also harbor glycine gatekeeper residues and are potentially capable of utilizing KTP $\gamma$ S. Moreover, this strategy could be extended to other CDPKs to identify their substrates and thereby define the pathways they control. Although other CDPKs are not directly amenable to this strategy, they can be engineered to gain sensitivity to both PP analogues and bulky ATP substrates. For example, when the endogenous allele of TgCDPK1 is replaced with one carrying a methionine gatekeeper, it provides a background for sensitizing other kinases to the PP analogues, thereby allowing study of the phenotypes they regulate.<sup>5</sup> In such an engineered background, it should also be possible to label the specific targets of other CDPKs using KTP $\gamma$ S to capture thiophosphorylated substrates, as has been done in other organisms.<sup>35,36</sup> Consequently, the approaches presented here provide a powerful opportunity for

defining the signaling pathways regulated by CDPKs within and across different apicomplexan parasites.

## METHODS

**Parasite Growth and Selection.** *T. gondii* tachyzoites were grown in human foreskin fibroblasts (HFF) cultured in complete medium [Dulbecco's Modified Eagles Medium (DMEM; Invitrogen) supplemented with 10% (v/v) tetracycline-free FBS (HyClone), 2 mM glutamine, 10 mM HEPES (pH 7.5), and 20  $\mu$ g mL<sup>-1</sup> gentamicin], as previously described.<sup>4</sup> When noted, parasites were selected by growth in complete medium containing ATc (1  $\mu$ g mL<sup>-1</sup>; Clontech) or pyrimethamine (3  $\mu$ M; Sigma).

**Plasmid and Strain Generation.** The TgCDPK1 cKO was described previously.<sup>4</sup> The  $\Delta$ ku80 $\Delta$ hxgprt background, referred to in this study as CDPK1<sup>G</sup> (provided by V. Carruthers, University of Michigan, USA), was used as a control and to generate the CDPK1<sup>M</sup> strain, as previously described.<sup>5</sup>

The tagging constructs for PRP-Ty and Ty-DrpB were directionally cloned PacI to AseI into *pLIC-YFP-HXGPRT* (provided by V. Carruthers, University of Michigan, USA). The 5'-UTR of DrpB was amplified (primers: 5'-GCG TTA ATT AAC CTC TTG CCG GAG C and 5'-GCG GCC GCG CCG AGA CGT CCT CGC GTT TGC CGT CAT CGA GCG GGT CCT GGT TCG TGT GGA CCT CCA TCT GCC GAA GAT TTC GGA GG) from RH genomic DNA and spliced at a NotI site with the DrpB cDNA amplified (primers: 5'-GAC GGC AAA CGC GAG GAC GTC and 5'-GCG GGC GCG CCT TAG TCG CTG AAC AGC GGA TTG TTC) from a library generated with the SMART cDNA synthesis kit (Clontech). The PRP 5'-UTR was amplified from RH genomic DNA (primers: 5'-GCG TTA ATT AAT GC A GCT TCG TGC GCA GCT CGA AG and 5'-CAC TGT TAT CCT CTA TTT TGA G) and spliced at a SacI site with the PRP cDNA amplified (primers: 5'-ATT CTG CTC CAG CGG TAG CGT G and 5'-GCG GGC GCG CCT TAA TCG AGC GGG TCC TGG TTC GTG TGG ACC TCC TCT TCG TCA TCA TCT TCG TCC G) from the library described above.

Stable lines expressing the tagged constructs were generated by selecting the transfected pool with the appropriate drug and isolating individual clones by limiting dilution. Clonal lines were maintained under pyrimethamine selection to prevent loss of the tagged alleles.

**Protein Purification and Kinase Assays.** Full-length TgCDPK1 was cloned and expressed as previously described.<sup>4</sup> Reactions were performed in a 20  $\mu$ L volume containing 0.5  $\mu$ g enzyme, 2  $\mu$ g dMBP (Millipore), 0.005% Tween-20 (v/v), 2 mM K<sub>2</sub>EGTA or 2 mM Ca<sup>2+</sup>-EGTA, 10 mM MgCl<sub>2</sub>, 1 mM analogue indicated (BioLog), 20 mM HEPES pH 7.5. Thiophosphorylation was allowed to proceed for 30 min at 30 °C. Laemmli sample buffer was added to each reaction and before resolving by SDS-PAGE and blotting. Total protein was imaged with SYPRO Ruby protein stain (Invitrogen) according to manufacturer's instructions.

**Thiophosphorylation and Target Identification.** Freshly lysed parasites were washed twice with ice-cold PBS and kept on ice until the kinase reactions were performed. Approximately 5  $\times$  10<sup>8</sup> parasites were used in a final reaction volume of 200  $\mu$ L. Reactions were performed in 1X D-PBS (Gibco) containing 2 mM K<sub>2</sub>EGTA or 2 mM CaEGTA (Molecular Probes), 10 mM MgCl<sub>2</sub>, 1% (v/v) NP-40, 1 mM GTP, 100  $\mu$ M ATP, 50  $\mu$ M KTP $\gamma$ S, 1X Phosphatase Inhibitor Cocktails I and II (EMD), and a protease inhibitor cocktail (E64, 1  $\mu$ g mL<sup>-1</sup>; AEBBSB, 10  $\mu$ g mL<sup>-1</sup>; TLCK, 10  $\mu$ g mL<sup>-1</sup>; leupeptin, 1  $\mu$ g mL<sup>-1</sup>; Sigma). Thiophosphorylation reactions were allowed to proceed for 30 min at 37 °C. Debris was removed by centrifugation at 20,000g, 10 min, 4 °C. Reactions were stopped by adding 4 mM EGTA, and alkylation was performed with 1 mM PNBM (Epitomics) for 2 h at RT. At this point samples for Western blotting were combined with Laemmli sample buffer and boiled.

Immunoprecipitation (IP) of thiophosphorylated proteins was performed as previously described.<sup>24</sup> In brief, PNBM was removed by buffer exchange with PD-10 columns (GE Healthcare), eluting proteins in an IP buffer containing 75 mM NaCl, 1% (v/v) NP-40, 1 mM EGTA, and 20 mM HEPES pH 7.5. Each sample was

immunoprecipitated with 10  $\mu\text{g}$  rabbit anti-thiophosphate ester (RmAb 51-8; Eptomics) immobilized on Protein G sepharose (Pierce). Following extensive washes with IP buffer, proteins were eluted from the beads by treating them with 20 mM DTT and 1% (v/v) RapiGest (Waters). A portion of the eluted proteins were analyzed by SDS-PAGE and stained with Oriole fluorescent gel stain (Bio Rad), according to manufacturer's instructions. The remaining samples were analyzed by mass spectrometry as described below.

Isolation of thiophosphorylated peptides was performed with samples that were not alkylated, according to the published protocol.<sup>26,37</sup> In brief, samples were digested with trypsin and added to 100  $\mu\text{L}$  of iodoacetyl-agarose beads (SulfoLink gel; Pierce) in 100  $\mu\text{L}$  of 50% (v/v) acetonitrile. Following overnight incubation, rotating in the dark, the beads were loaded into a disposable column and washed with 2 mL each of water, 5 M NaCl, 50% (v/v) acetonitrile, and 5% (v/v) formic acid in water. Peptides were eluted with 500  $\mu\text{L}$  of a 1 mg  $\text{mL}^{-1}$  solution of Oxone (Sigma) and concentrated with  $\text{C}_{18}$  Ziptips. Samples were analyzed by LC-MS/MS with an LTQ-Orbitrap Velos, with data searched using the ToxoDB 6.1 database of *T. gondii* proteins. Mass spectrometry was performed at the Danforth Plant Science Center's Proteomics & Mass Spectrometry Facility (St. Louis, MO). Data analysis, performed using Scaffold (Proteome Software), was restricted to proteins for which at least two spectra had been assigned with a probability greater than 90% and which had been identified with at least two peptides in the combined set of samples. This included proteins identified with a single phosphorylation site in the peptide capture approach, as long as a different peptide had been identified in the IP experiment and at least two spectra had been assigned to the phosphopeptide.

**Sequence Analysis.** To determine protein homology between different apicomplexan genome, we used OrthoMCL DB version 5, as previously described.<sup>31</sup>

**Motif Analysis.** The sequence preference of TgCDPK1 was measured by phosphorylating a positional scanning peptide array as previously described<sup>28</sup> for 2 h at 30 °C with 1 ng  $\text{mL}^{-1}$  recombinant TgCDPK1 in 50 mM HEPES, pH 7.4, 10 mM  $\text{MgCl}_2$ , 2 mM Ca-EGTA, 0.1% (v/v) Tween 20, 50  $\mu\text{M}$  [ $\gamma$ -<sup>33</sup>P]-ATP (33  $\mu\text{Ci mL}^{-1}$ ). The normalized values from the peptide array were used to create a Gribskov protein profile suitable for use with *Prophet* available from EMBOSS.<sup>38</sup> Each of the proteins identified in the peptide capture experiment was searched using the TgCDPK1 profile to determine the rank preference of different 10-letter peptides along the protein, centered on all possible Ser and Thr residues. Data for other phosphorylation sites present in these proteins was based on the published *T. gondii* global phosphoproteome<sup>29</sup> and obtained from ToxoDB.<sup>20</sup> The TgCDPK1 profile and the 10-letter peptides carrying the sites identified as thiophosphorylated were submitted to WebLogo,<sup>39</sup> to generate the visual representations of the preference motifs.

**Immunofluorescence Microscopy.** Immunofluorescence staining was performed as described previously<sup>40</sup> following permeabilization with 0.1% (w/v) saponin (Sigma) with mouse-anti-Ty (mAb BB2)<sup>41</sup> and rabbit anti-ALD1,<sup>42</sup> followed by Alexa488-goat anti-mouse IgG (Invitrogen) and Alexa594-goat anti-rabbit IgG (Invitrogen). Images were acquired in a Zeiss Axioskop fluorescence microscope equipped with a 63X 1.3 numerical aperture lens and an AxioCam MRm camera (Carl Zeiss).

**Immunoprecipitation and Western Blotting.** Immunoprecipitation of Ty-tagged proteins was performed following thiophosphorylation and alkylation as described above. Protein G sepharose (Pierce) was bound to mouse-anti-Ty (mAb BB2)<sup>41</sup> 1 h, washed with IP buffer, and incubated with samples overnight at 4 °C. Following extensive washes with IP buffer, Laemmli sample buffer containing 2-mercaptoethanol (3% final concentration) was added to each sample, before boiling for 10 min.

Parasite lysates ( $\sim 10^7$  cells per lane) were resolved by SDS-PAGE, transferred to nitrocellulose membranes, and blotted with rabbit anti-TgALD1, rabbit anti-thiophosphate ester (RmAb 51-8; Eptomics), mouse anti-Ty (mAb BB2),<sup>41</sup> or mouse anti-GRA1 (mAb Tg17-43, kindly provided by Marie France Cesbron, Genoble, France). The

signals were detected using IRDye 680CW conjugated donkey anti-rabbit IgG (LI-COR Biosciences) and IRDye 800CW conjugated goat anti-mouse IgG (LI-COR Biosciences) on the Odyssey infrared imager (LI-COR Biosciences). Images were processed and analyzed using the Odyssey infrared imaging system software.

**Radiolabeling Assays.** For *in vivo* labeling, extracellular parasites were incubated in phosphate-free DMEM (Gibco) with 1 mCi [<sup>32</sup>P] orthophosphate (specific activity, 8500 Ci  $\text{mmol}^{-1}$ ; Perkin-Elmer) for 1 h at 37 °C, 5%  $\text{CO}_2$ . Labeled parasites were resuspended in media alone or supplemented with 3% (v/v) FBS and 2% (v/v) EtOH and incubated for 5 min at 37 °C. Cells were resolved by SDS-PAGE and Western blotted, following the procedures above. Radiolabel was imaged with an FLA5000 phosphorimager (Fuji).

## ■ ASSOCIATED CONTENT

### Supporting Information

This material is available free of charge via the Internet at <http://pubs.acs.org>

## ■ AUTHOR INFORMATION

### Corresponding Author

\*E-mail: [sibley@wustl.edu](mailto:sibley@wustl.edu).

### Present Address

<sup>§</sup>Whitehead Institute for Biomedical Research, Cambridge, MA 02142, USA.

### Notes

The authors declare no competing financial interest.

## ■ ACKNOWLEDGMENTS

We thank N. Hertz and K. Shokat for helpful technical advice, M. Treeck and J. Boothroyd for sharing unpublished data, M-F. Cesbron for providing antibodies, V. Carruthers for the  $\Delta ku80\Delta hxxprt$  line and pLIC plasmids, S. Alvarez for performing the mass spectrometry, K. Tang and J. Barks for technical assistance, and M. Meissner and O. Billker for helpful discussions. This work was supported in part by a predoctoral fellowship from the American Heart Association (S.L.) and a grant from the National Institutes of Health AI034036 (L.D.S.)

## ■ REFERENCES

- (1) Hall, S., Ryan, K. A., and Buxton, D. (2001) The epidemiology of toxoplasma infection, in *Toxoplasmosis: A comprehensive clinical guide* (Joynson, D. H., and Wreghitt, T. J., Eds.), pp 58–124, Cambridge University Press, New York.
- (2) World Health Organization (2011) *World Malaria Report 2010*, World Health Organization, Geneva.
- (3) Billker, O., Lourido, S., and Sibley, L. D. (2009) Calcium-dependent signaling and kinases in apicomplexan parasites. *Cell Host Microbe* 5, 612–622.
- (4) Lourido, S., Shuman, J., Zhang, C., Shokat, K. M., Hui, R., and Sibley, L. D. (2010) Calcium-dependent protein kinase 1 is an essential regulator of exocytosis in *Toxoplasma*. *Nature* 465, 359–362.
- (5) Lourido, S., Tang, K., and Sibley, L. D. (2012) Distinct signalling pathways control *Toxoplasma* egress and host-cell invasion. *EMBO J.* 31, 4524–4534.
- (6) Dvorin, J. D., aMartyn, D. C., Patel, S. D., Grimley, J. S., Collins, C. R., Hopp, C. S., Bright, A. T., Westenberger, S., Winzeler, E., Blackman, M. J., Baker, D. A., Wandless, T. J., and Duraisingh, M. T. (2010) A plant-like kinase in *Plasmodium falciparum* regulates parasite egress from erythrocytes. *Science* 328, 910–912.
- (7) Sibley, L. D. (2004) Intracellular parasite invasion strategies. *Science* 304, 248–253.
- (8) Morrisette, N. S., Murray, J. M., and Roos, D. S. (1997) Subpellicular microtubules associate with an intramembranous particle lattice in the protozoan parasite *Toxoplasma gondii*. *J. Cell Sci.* 110 (Pt 1), 35–42.

- (9) Carruthers, V. B., Moreno, S. N. J., and Sibley, L. D. (1999) Ethanol and acetaldehyde elevate intracellular  $[Ca^{2+}]$  calcium and stimulate microneme discharge in *Toxoplasma gondii*. *Biochem. J.* 342, 379–386.
- (10) Lovett, J. L., and Sibley, L. D. (2003) Intracellular calcium stores in *Toxoplasma gondii* govern invasion of host cells. *J. Cell Sci.* 116, 3009–3016.
- (11) Battaini, F., and Pascale, A. (2005) Protein kinase C signal transduction regulation in physiological and pathological aging. *Ann. N.Y. Acad. Sci.* 1057, 177–192.
- (12) Skelding, K. A., and Rostas, J. A. (2012) The role of molecular regulation and targeting in regulating calcium/calmodulin stimulated protein kinases. *Adv. Exp. Med. Biol.* 740, 703–730.
- (13) Nagamune, K., and Sibley, L. D. (2006) Comparative genomic and phylogenetic analyses of calcium ATPases and calcium-regulated proteins in the Apicomplexa. *Mol. Biol. Evol.* 23, 1613–1627.
- (14) Harper, J. F., and Harmon, A. C. (2005) Plants, symbiosis and parasites: a calcium signalling connection. *Nat. Rev. Mol. Cell Biol.* 6, 555–566.
- (15) Billker, O., Dechamps, S., Tewari, R., Wenig, G., Franke-Fayard, B., and Brinkmann, V. (2004) Calcium and a calcium-dependent protein kinase regulate gamete formation and mosquito transmission in a malaria parasite. *Cell* 117, 503–514.
- (16) Siden-Kiamos, I., Ecker, A., Nyback, S., Louis, C., Sinden, R. E., and Billker, O. (2006) *Plasmodium berghei* calcium-dependent protein kinase 3 is required for ookinete gliding and mosquito midgut invasion. *Mol. Microbiol.* 60, 1355–1363.
- (17) Ishino, T., Orito, Y., Chinzei, Y., and Yuda, M. (2006) A calcium-dependent protein kinase regulates *Plasmodium* ookinete access to the midgut epithelial cell. *Mol. Microbiol.* 59, 1175–1184.
- (18) Coppi, A., Tewari, R., Bishop, J. R., Bennett, B. L., Lawrence, R., Esko, J. D., Billker, O., and Sinnis, P. (2007) Heparan sulfate proteoglycans provide a signal to *Plasmodium* sporozoites to stop migrating and productively invade host cells. *Cell Host Microbe* 2, 316–327.
- (19) Barclay, J. W., Morgan, A., and Burgoyne, R. D. (2005) Calcium-dependent regulation of exocytosis. *Cell Calcium* 38, 343–353.
- (20) database: <http://ToxoDB.org>.
- (21) Wernimont, A. K., Artz, J. D., Finerty, P., Lin, Y., Amani, M., Allali-Hassani, A., senisterra, G., Vedadi, M., Tempel, W., Mackenzie, F., Chau, I., Lourido, S., Sibley, L. D., and Hui, R. (2010) Structures of apicomplexan calcium-dependent protein kinases reveal mechanism of activation by calcium. *Nat. Struct. Mol. Biol.* 17, 596–601.
- (22) Ojo, K. K., Larson, E. T., Keyloun, K. R., Castaneda, L. J., DeRoucher, A. E., Klnampudi, K. K., Kim, J. E., Arakaki, T. L., Murphy, R. C., Zhang, L., Napuli, A. J., Maly, D. J., Verlinde, C. L. M. J., Buckner, F. S., Parsons, M., Hol, W. G. J., Meritt, E. A., and Van Voorhis, C. (2010) *Toxoplasma gondii* calcium-dependent protein kinase 1 is a target for selective kinase inhibitors. *Nat. Struct. Mol. Biol.* 17, 602–607.
- (23) Sugi, T., Kato, K., Kobayashi, K., Watanabe, S., Kurokawa, H., Gong, H., Pandey, K., Takemae, H., and Akashi, H. (2010) Use of the kinase inhibitor analog INM-PP1 reveals a role for *Toxoplasma gondii* CDPK1 in the invasion step. *Eukaryotic Cell* 15, 1716–1725.
- (24) Allen, J. J., Li, M., Brinkworth, C. S., Paulson, J. L., Wang, D., Hubner, A., Chou, W. H., Davis, R. J., Burlingame, A. L., Messing, R. O., Katayama, C. D., Hedrick, S. M., and Shokat, K. M. (2007) A semisynthetic epitope for kinase substrates. *Nat. Methods* 4, 511–516.
- (25) Witucki, L. A., Huang, X., Shah, K., Liu, Y., Kyin, S., Eck, M. J., and Shokat, K. M. (2002) Mutant tyrosine kinases with unnatural nucleotide specificity retain the structure and phospho-acceptor specificity of the wild-type enzyme. *Chem. Biol.* 9, 25–33.
- (26) Blethrow, J. D., Glavy, J. S., Morgan, D. O., and Shokat, K. M. (2008) Covalent capture of kinase-specific phosphopeptides reveals Cdk1-cyclin B substrates. *Proc. Natl. Acad. Sci. U.S.A.* 105, 1442–1447.
- (27) Huynh, M. H., and Carruthers, V. B. (2009) Tagging of endogenous genes in a *Toxoplasma gondii* strain lacking Ku80. *Eukaryotic Cell* 8, 530–539.
- (28) Turk, B. E., Hutti, J. E., and Cantley, L. C. (2006) Determining protein kinase substrate specificity by parallel solution-phase assay of a large number of peptide substrates. *Nat. Protoc.* 1, 375–379.
- (29) Treeck, M., Sanders, J. L., Elias, J. E., and Boothroyd, J. C. (2011) The phosphoproteomes of *Plasmodium falciparum* and *Toxoplasma gondii* reveal unusual adaptations within and beyond the parasites' boundaries. *Cell Host Microbe* 10, 410–419.
- (30) Breinich, M. S., Ferguson, D. J. P., Foth, B. J., van Dooren, G. G., Lebrun, M., Quon, D. V., Striepen, B., Bradley, P. J., Frischknecht, F., Carruthers, V. B., and Meissner, M. (2009) A dynamin is required for the biogenesis of secretory organelles in *Toxoplasma gondii*. *Curr. Biol.* 19, 277–286.
- (31) Chen, F., Mackey, A. J., Stoeckert, C. J., Jr., and Roos, D. S. (2006) OrthoMCL-DB: Querying a comprehensive multi-species collection of ortholog groups. *Nucleic Acids Res.* 34, D363–368.
- (32) van Dooren, G. G., Reiff, S. B., Tomova, C., Meissner, M., Humbel, B. M., and Striepen, B. (2009) A novel dynamin-related protein has been recruited for apicoplast fission in *Toxoplasma gondii*. *Curr. Biol.* 19, 267–276.
- (33) Jaiswal, J. K., Rivera, V. M., and Simon, S. M. (2009) Exocytosis of post-Golgi vesicles is regulated by components of the endocytic machinery. *Cell* 137, 1308–1319.
- (34) Anantharam, A., Bittner, M. A., Aikman, R. L., Stuenkel, E. L., Schmid, S. L., Axelrod, D., and Holz, R. W. (2011) A new role for the dynamin GTPase in the regulation of fusion pore expansion. *Mol. Biol. Cell* 22, 1907–1918.
- (35) Böhmer, M., and Romeis, T. (2007) A chemical-genetic approach to elucidate protein kinase function in planta. *Plant Mol. Biol.* 65, 817–827.
- (36) Carlson, S. M., Chouinard, C. R., Labadorf, A., Lam, C. J., Schmelzle, K., Fraenkel, E., and White, F. M. (2011) Large-scale discovery of ERK2 substrates identifies ERK-mediated transcriptional regulation by ETV3. *Sci. Signaling* 4, rs11.
- (37) Hertz, N. T., Wang, B. T., Allen, J. J., Zhang, C., Dar, A. C., Burlingame, A. L., and Shokat, K. M. (2010) Chemical genetic approach for kinase-substrate mapping by covalent capture of thiophosphopeptides and analysis by mass spectrometry. *Curr. Protoc. Chem. Biol.* 2, 15–36.
- (38) Rice, P., Longden, I., and Bleasby, A. (2000) EMBOSS: The European molecular biology open software suite. *Trends Genetics* 16, 276–277.
- (39) Crooks, G. E., Chandonia, J. M., and Brenneer, S. E. (2004) WebLogo: a sequence logo generator. *Genome Res.* 14, 1188–1190.
- (40) Starnes, G. L., Coincon, M., Sygusch, J., and Sibley, L. D. (2009) Aldolase is essential for energy production and bridging adhesin-actin cytoskeletal interactions during parasite invasion of host cells. *Cell Host Microbe* 5, 353–364.
- (41) Bastin, P., Bagherzadeh, Z., Matthews, K. R., and Gull, K. (1996) A novel epitope tag system to study protein targeting and organelle biogenesis in *Trypanosoma brucei*. *Mol. Biochem. Parasitol.* 77, 235–239.
- (42) Starnes, G. L., Jewett, T. J., Carruthers, V. B., and Sibley, L. D. (2006) Two separate, conserved acidic amino acid domains within the *Toxoplasma gondii* MIC2 cytoplasmic tail are required for parasite survival. *J. Biol. Chem.* 281, 30745–30754.